Green Chemistry

PAPER

View Article Online
View Journal | View Issue

Cite this: *Green Chem.*, 2021, **23**, 2079

Efficient extracellular laccase secretion *via* bio-designed secretory apparatuses to enhance bacterial utilization of recalcitrant lignin†

Lanfang Cao,‡[a] Lu Lin, *‡[b] Haiyan Sui,[c] Heng Wang,[d] Zhichao Zhang,[d] Nianzhi Jiao[e,f] and Jizhong Zhou[g]

Microbial-driven lignin conversion has a significant impact on the biogeochemistry of global ecosystems and biomass utilization. During this process, secretion of extracellular ligninolytic enzymes is the first, essential step, yet there is a significant challenge to the secretion of these high-redox potential enzymes in bacteria, especially in Gram-negative bacteria. In this study, genome and proteome analyses enabled us to bio-design two types of extracellular secretory apparatus, both of which effectively secreted a heterologous laccase in *Pseudomonas putida*, up to ~300 U mL^{-1}. Importantly, a strong cooperation between *P. putida* A514 cells and the extracellular laccase, which was either released to the medium or displayed on the cell surface, was observed to significantly promote cell growth (9×10^{10} CFUs mL^{-1}) and lignin consumption (12.5%). Chemical analyses of lignin further confirmed the effect on lignin utilization. Moreover, we demonstrated that a free laccase-A514 cell system exhibited greater effect on lignin utilization than that of a cell-immobilized laccase complex, which challenges the current view of bacterial polymer catabolism, and suggests the importance of secretory pathways and sufficient reaction surface for lignin biocatalysis. Our study advances the knowledge of secretion mechanisms in Gram-negative bacteria and provides novel insights into the lignin utilization by extracellular lignolytic enzyme-bacterial cell systems.

Received 2nd December 2020,
Accepted 5th February 2021

DOI: 10.1039/d0gc04084c

rsc.li/greenchem

1 Introduction

Lignin is a complex, heterogeneous, phenylpropanoid polymer.[1] As one of the most abundant natural organic compounds on Earth, lignin has a significant impact on the biogeochemistry of global ecosystems and biomass utilization. Although it is the most recalcitrant component of terrestrially derived organic carbon, microorganisms, including white-rot fungi and bacteria, have evolved the capacity to degrade lignin to complete global carbon cycling.[2] Using various extracellular enzymes, they first break down the particulate substrates to a low-molecular weight compounds and then these are actively transported across cell walls for further catabolism.[1,3,4] Thus, extracellular enzymes are essential in the heterotrophic remineralization of organic carbon[5,6] and are either released freely into solution or remain tethered to the cell.[1] Cells that produce extracellular enzymes may prefer to retain secreted enzymes at the cell surface, as this means that metabolites are generated close to the cell and can be readily taken up. In contrast, entire microbial communities may profit from the activity of enzymes that are released in the environment.[7,8] Both strategies have been observed in microbial cellulose degradation. Aerobic fungi usually secrete different cellulolytic components to hydrolyze cellulose, while some anaerobic bacteria produce cell-bound cellulosomes for cellulose hydrolysis.[9,10] It is interesting to note that anaerobic cellulolytic bacteria can rapidly and effectively hydrolyze cellulose with much lower levels of secretory cellulase production than fungi.[11] Several studies also reported that bio-designed cellulosomes exhibited a higher hydrolysis rate than their noncom-

[a]*Ocean College, Zhejiang University, Hangzhou, China*
[b]*Institute of Marine Science and Technology, Shandong University, Qingdao 266237, China. E-mail: linlu2019@sdu.edu.cn*
[c]*State Key Laboratory of Microbial Technology, Shandong University, Qingdao 266237, China*
[d]*Key Laboratory of Health Risk Factors for Seafood of Zhejiang Province, Zhoushan Municipal Center for Disease Control and Prevention, Zhoushan, Zhejiang, China*
[e]*State Key Laboratory of Marine Environmental Science and College of Ocean and Earth Sciences, Xiamen University, Xiamen 361005, China*
[f]*Joint Lab for Ocean Research and Education at Shandong University, Xiamen University and Dalhousie University, Qingdao, China*
[g]*Institute for Environmental Genomics, Department of Microbiology and Plant Biology, and School of Civil Engineering and Environmental Sciences, University of Oklahoma, Norman, OK, USA*

†Electronic supplementary information (ESI) available: S1: Supplementary tables, S2: Supplementary figures. See DOI: 10.1039/d0gc04084c

‡These authors contributed equally to this work.

plexed counterparts which contain the same enzymes as the cellulosomes, yet in the free form.[12,13] Unlike the cellulose hydrolysis process, enzymatic lignin degradation primarily depends on redox reactions.[14] Secretory production of ligninolytic enzymes, which change the redox environment within the cell is, hence, highly challenging. Moreover, in contrast to the wealth of biochemical knowledge on cellulose hydrolysis, lignin oxidation has not as yet been fully characterized.[14–17] Whether, and how, cell-bound ligninolytic enzymes show a higher catalytic rate than cell-free ligninolytic enzymes is largely unknown.

Several bacteria have been identified as capable of delignification.[18,19] Among them, members of the *Pseudomonas*, a genus of Gram-negative bacteria, have recently been used to establish the concept of bacterial lignin conversion.[20–22] However, their efficiency of lignin degradation is relatively lower than that of their fungal counterparts,[18,19] as limited extracellular secretion capacity represented a major hurdle in bacterial lignin conversion.[23,24] Previous study attempted to enhance extracellular secretion capacity of ligninolytic enzymes.[20] For example, a N-terminal signal peptide (*e.g.*, pelB and oprI) was employed for the extracellular production of recombinant multifunctional dye peroxidase (DyP2) in *P. putida*.[20] The results showed that pelB guided DyP2 only across the inner membrane, causing weak extracellular DyP2 activity through leakage from the periplasmic space.[20] It suggested that, unlike Gram-positive bacteria, due to the existence of both inner and outer members, there is an inherent challenge to ligninolytic enzyme secretion in Gram-negative bacteria,[25] even though extracellular secretion mechanisms in Gram-negative bacteria have been extensively studied.[26,27] Moreover, the ligninolytic performances of enzymes that are either displayed on the cell surface or released to extracellular space were not investigated and compared. Hence, systematic understanding of the protein secretion mechanism involved and investigation of the synergistic lignin conversion effect is essential in bacteria to overcome lignin's recalcitrance.

In this study, we employed laccase from *Streptomyces coelicolor* A3[28] as the model protein to investigate the efficient extracellular protein production in *P. putida*. The small laccase was targeted, as (i) *P. putida* A514[23] lacks a native laccase with ligninolytic activity and (ii) unlike peroxidases, laccases do not require the presence of H_2O_2 to catalyze lignin oxidation.[14] Genome and proteome analyses were carried out to investigate the secretion systems in *P. putida*. These findings enabled us to design two laccase secretion apparatuses *via* Type I and Type V secretion systems to either release laccase in medium or display it on cell surface, respectively. Moreover, the effects on lignin utilization of immobilized laccase-A514 and free laccase-A514 were compared, and suggested that the free laccase-A514 system exhibited higher cell growth and lignin consumption. This study not only improved extracellular secretion capacity in *P. putida*, but also provided insights to enhance bacterial enzymatic lignin utilization.

2 Result

2.1 Intracellular expression of heterologous laccase in *P. putida* A514 cell

For extracellular laccase production in *P. putida* A514, functional expression of the intracellular laccase was investigated first. For this purpose, the codon optimized laccase gene (from *S. coelicolor* A3), driven by inducible promoter P_{xylA},[29] was inserted into the plasmid pPROBE-GT to construct the plasmid pGlac. It was subsequently transformed into *P. putida* A514, generating the recombinant strain A_{pGlac} (Table S1†). SDS-PAGE analysis identified the 34.6 kDa protein band within soluble cell lysis samples of A_{pGlac}, while it was absent in the control strain A_{pGT} (Fig. S1†). The subsequently detected intracellular laccase activity in A_{pGlac} (~0.73 U mL^{-1} of cell culture) validated that the heterologous laccase can be functionally expressed in *P. putida* A514. It was further enhanced *via* optimization of various conditions, including pH, metal ions, temperature, shaker speed, incubation time, and expression vectors, resulting in a 143-fold increase in A_{pULac}, from ~0.7 to 100 U mL^{-1} (Table S2†).

2.2 Extracellular laccase expression *via* the bio-designed Type I secretion apparatus

In *Pseudomonas* species, the secretory mechanism of lipase (TliA) has been well-characterized. The ATP-binding cassette (ABC) transporter (AprDEF) recognizes the C-terminal signal sequence of TliA and transports it to extracellular space *via* the Type I secretion system (TISS).[30,31] Furthermore, its C-terminal signal sequence (LARD3) and AprDEF in *P. fluorescens* no. 33 have been developed to be a secretion apparatus of recombinant proteins in Gram-negative bacteria (*e.g.*, *E. coli* and *Pseudomonas* strains).[32,33] Hence, the homologous gene cluster (*aprDEF* and *tliA*) was blasted and, as expected, identified in *P. putida* A514 genome (Fig. 1A).[20,34] As a result, laccase combined with the C-terminal signal peptide of TliA was expressed in A514. Meanwhile, to enhance the capacity of the secretory system, AprDEF, the key components for the ABC transporter machinery, were overexpressed, generating the recombinant strain $A_{pUI\text{-}2539}$ (Fig. 1A and Table S1†).

Unexpectedly, extracellular laccase activity was not observed in the culture medium of $A_{pUI\text{-}2539}$, although intracellular activity was detected (Fig. 1B and Fig. S2A†). This suggested an incompatibility between the laccase and the signal peptide of TliA. Therefore, as an alternative, the C-terminal signal sequence of *aprA*, encoding alkaline protease, was targeted, as AprA and TliA are both transported by AprDEF[33,34] (Fig. 1A). Consequently, extracellular laccase activity (2.85 U mL^{-1} of cell culture) was detected in the culture medium of the recombinant strain $A_{pUI\text{-}2549}$, validating that laccase can be secreted to the culture medium *via* TISS (Fig. 1B).

Next, the extracellular laccase activity was optimized at the transcriptional, translational, and protein folding levels. (i) To optimize laccase transcription, 2 mM xylose was introduced at different time points (0, 8, and 14 hours) to activate the xylose inducible promoter P_{xylA} (Fig. 1C). A two-fold increase of extra-

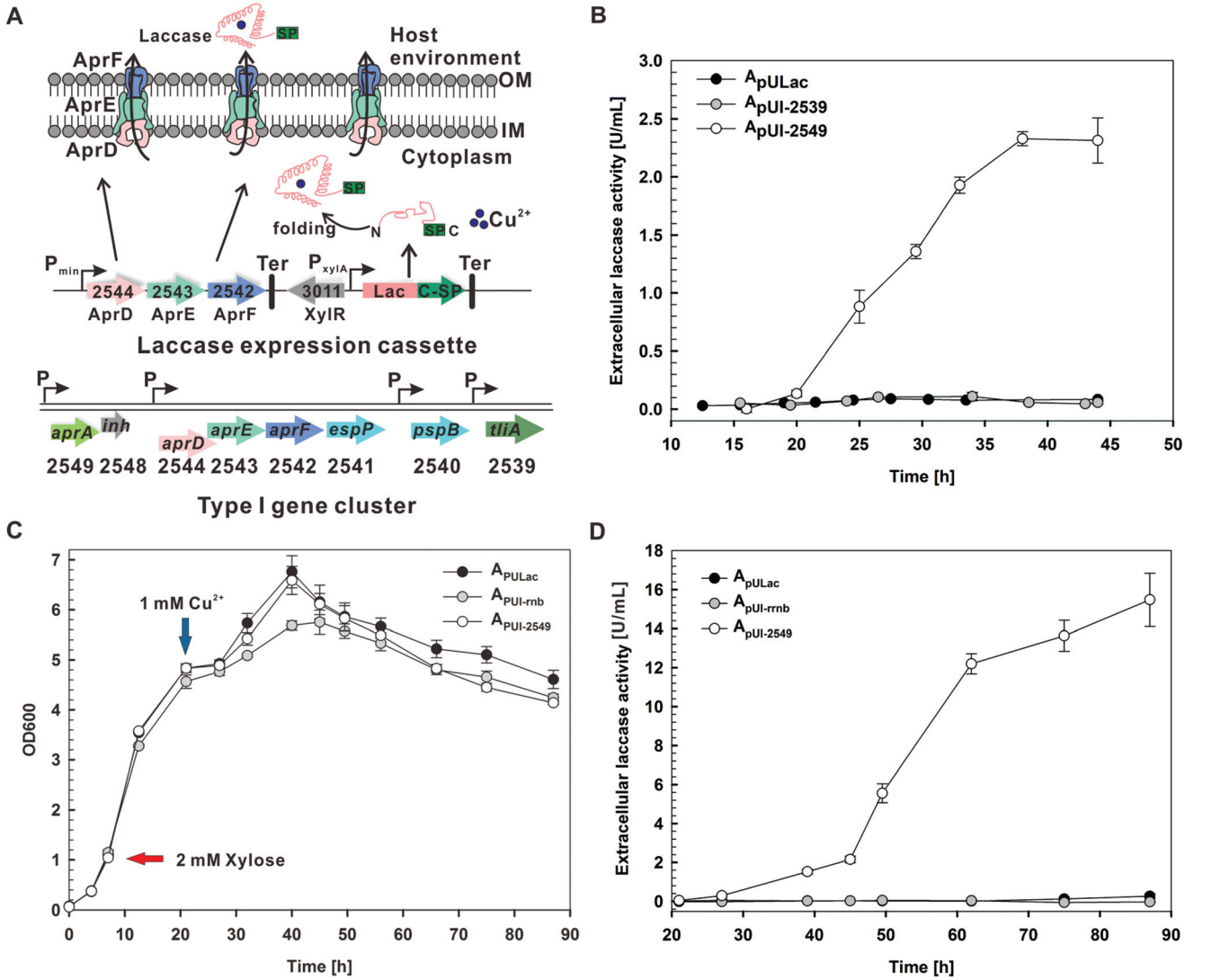

Fig. 1 Biodesign of the TISS to secrete laccase. (A) Graphic overview of extracellular production free laccase *via* the bio-designed TISS. Organization of bio-designed TISS is presented. P: promoter, SP: signal peptide, Ter: transcriptional terminator, XylR: regulator of the P_{xylA} promoter. (B) Real-time extracellular laccase activities for the recombinant A514 strains with laccase integrated using different C-terminal signal peptides in TISS. (C) The growth curve of $A_{pUI-2549}$. The red arrow indicates time point at which 2 mM xylose was added, while the blue arrow represents the time point at which 1 mM Cu^{2+} was added. (D) The optimized extracellular laccase activities of $A_{pUI-2549}$. A_{pULac} without any signal peptide and ApUI-rnb without laccase gene were used as the reference strains.

cellular laccase activity (5.7 U mL^{-1}) was detected, when xylose was added at 8 hours (Table S3 and Fig. S2C†), although similar growth curves were observed among the three $A_{pUI-2549}$ cultures (Fig. S2B†). (ii) Three key cultivation parameters were optimized to improve laccase expression, including incubation time, agitation rates, and temperature. As a result, 8.4 U mL^{-1} extracellular laccase was reached (Table S3†). (iii) Copper ion is known to be the most critical metal ion for laccase activity, even though it can be toxic to cell growth.[35] Thus, to minimize the toxicity, $CuSO_4$ should be added at the proper time. Three time points (0, 22, and 44 h) were investigated and the highest extracellular laccase activity (15.5 U mL^{-1}) was achieved when it was added at 22 hours (Fig. 1C, D and Table S3†).

2.3 Displaying laccase on the *P. putida* A514 cell surface *via* the bio-designed Type V secretion machinery

Via the bio-designed Type I secretion apparatus, laccase was secreted in a single process, without a periplasmic intermediate (Fig. 1A). It also could be secreted in a two-step process, *via* cytoplasmic membrane translocation and extracellular secretion (Fig. 2A).[27]

For cytoplasmic membrane translocation, genome analysis suggested that SecB-dependent pathway and Tat (twin-arginine translocation) pathway, both of which are commonly strategies,[7,36] were present in *P. putida* A514. Considering that known secreted laccase proteins are primarily secreted *via* the

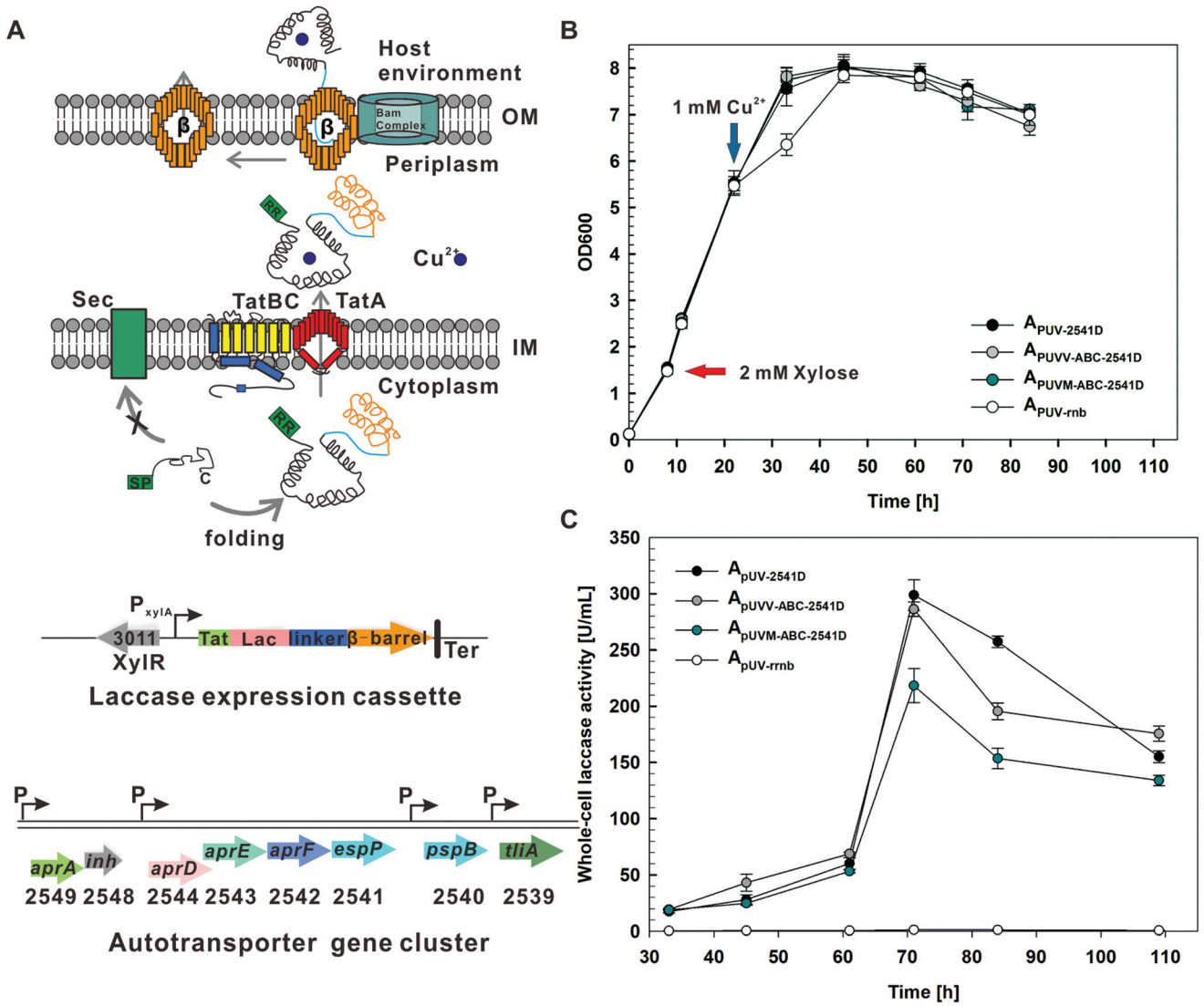

Fig. 2 Biodesign of the AT in TVSS to secrete laccase. (A) Graphic overview of production cell-bound laccase *via* the bio-designed AT in TVSS. Organization of bio-designed AT is presented. The tat signal sequence (RR), represented in green, is a native Tat signal peptide in A514. The passenger domain, in pink, is laccase protein with the linker region in blue and the β domain in yellow at the C-terminus. P: promoter, Ter: transcriptional terminator, XylR: regulator of the P_{xylA} promoter. (B) The growth curves of $A_{pUV\text{-}2541D}$, $A_{pUVV\text{-}ABC\text{-}2541D}$, $A_{pUVM\text{-}ABC\text{-}2541D}$, and $A_{pUV\text{-}rnb}$. The red arrow indicates time point at which 2 mM xylose was added, while the blue arrow represents the timepoint at which 1 mM Cu^{2+} was added. (C) The optimized whole-cell laccase activities of $A_{pUV\text{-}2541D}$, $A_{pUVV\text{-}ABC\text{-}2541D}$, and $A_{pUVM\text{-}ABC\text{-}2541D}$.

Tat protein transport system,[28,37] fifteen putative Tat signal peptides in A514, predicted by both TatP and TatFind software,[38] were selected. A refined subset of seven signal peptides were further targeted through information gleaned from the protein location prediction (http://www.pseudomonas.com/) and secretome of A514,[20] and were then respectively fused with the laccase protein in the A514 strain. Of the seven recombinant strains, three (A_{pG1543}, A_{pG2816} and A_{pG4529}) showed positive periplasmic laccase activity, with A_{pG2816} showing the highest activity (16.65 U mL^{-1}, Fig. S3A and Table S4†). As a result, the laccase expression and secretion system in A_{pG2816} was investigated to enhance periplasmic activity. A high copy number expression vector (pUCP18-Gm)[23] was used to enhance the laccase expression level, which resulted in a threefold increase of periplasmic laccase activity (49.16 U mL^{-1}, Table S4†). On the other hand, the capacity of Tat protein secretory system is commonly a limitation for the efficient secretion of heterologous proteins.[39] Thus, the key components in the machinery, *tatABC*, were overexpressed. Two *tatABC* expression cassettes driven by different strength promoters, P_{min}::*tatABC* and P_{van}::*tatABC*, were introduced in A_{pU2816}, generating the recombinant strains, $A_{pUM\text{-}ABC\text{-}2816}$ and $A_{pUV\text{-}ABC\text{-}2816}$, respectively. However, A_{pU2816}, $A_{pUM\text{-}ABC\text{-}2816}$, and $A_{pUV\text{-}ABC\text{-}2816}$ all showed similar periplasmic laccase activity ($p > 0.05$), suggesting the *tatABC* expression level wasn't the rate-limiting step for the periplasmic laccase secretion (Table S4†).

For extracellular secretion, autotransporters (ATs) of the Type V secretion system (TVSS) were investigated, because the classical AT carry all elements for translocation across the periplasm and outer membrane within each protein itself, including a N-terminal Sec signal peptide, a passenger domain that carries the effector function of the AT, and a C-terminal pore forming β-domain.[40,41] Among the three domains, the β-domain, which integrates into the OM, is responsible for translocation of the passenger into the extracellular space (Fig. 2A). Four homologous proteins of EspP (serine proteases) and EstA (lipolytic enzymes), both of which are well-characterized ATs,[42–44] were identified in A514. Therefore, their C-terminal regions, including linkers and β-domains, were cloned into the vectors for laccase OM transportation (Fig. 2A). As a result, laccase activities were detected by the whole-cell laccase activity assay (Fig. S3B†), suggesting that the laccase was displayed on the cell surface, covalently associated with the β-domain (Fig. 2A). Furthermore, it also revealed that all of the tested C-terminal regions could mediate laccase across the OM. Among them, $A_{pUV2541A}$ displayed the highest activity, 15.99 U mL^{-1} (Fig. S3B†). Hence, its cell-bound laccase activity was further optimized. First, the C-terminal linkers of $A_{pUV2541A}$ were investigated to improve the bio-designed secretion system. It's worth noting that the linker region, connecting the passenger and β-domains, is important for outer membrane translocation of its passenger.[45,46] The 2541A linker region was sequentially deleted, generating four linker regions of different lengths (Fig. S4A and B†). The results suggested that 2514D, containing the shortest length of linker, had enhanced laccase secretion efficiency (Fig. S4C†) and further increased the extracellular laccase activity by 50% (23.42 U mL^{-1}, Fig. S4D†), validating the role of the linker in extracellular laccase secretion (Table S4†). Second, similar to TISS, extracellular laccase activity was also improved at the transcriptional, translational, and protein folding levels, respectively (Table S4†). Consequently, the activity was increased another 13-fold, achieving ~300 U mL^{-1} (Fig. 2B, C and Table S4†). Third, overexpression of *tatABC* was also tested, suggesting that enhanced *tatABC* expression didn't contribute to OM secretion of laccase (Fig. 2C and Table S4†).

2.4 Integration of laccase secretion module promoted *P. putida* A514 cell growth as well as lignin utilization

As previously reported, bacterial laccases promote lignin oxidation and improve cell growth on lignin[24,35] (Fig. S5†), although laccases are believed to have roles in lignin synthesis in plants, cell pigment formation and metal oxidation in microorganisms.[28] Therefore, the cell growth and lignin utilization of $A_{pUI-2549}$ and $A_{pUV-2541D}$, were investigated, while A_{pU} was used as the reference strain. Considering poor cell growth would limit laccase production and secretion, the strain cultivation conditions in the presence of lignin were firstly optimized by the classical one variable at a time (OVAT) method, including inoculum sizes, different concentrations of $CuSO_4$, NH_4Cl, xylose, and yeast extract, as well as addition time points of $CuSO_4$ (Table S5†). Consequently, A_{pU} reached 3.3×10^{10} CFUs mL^{-1} from the initial 6.8×10^3 CFUs mL^{-1} after 72 h cultivation in lignin rich medium, according to the CFU (Colony Forming Unit) assay (Fig. 3A). Furthermore, $A_{pUI-2549}$ exhibited significant growth improvement, ~2.7-fold enhancement over the control, A_{pU} ($p < 0.05$). Similarly, $A_{pUV-2541D}$ also showed ~2.5-fold higher than A_{pU} in lignin rich medium ($p < 0.05$, Fig. 3A and Table S5†). Subsequently, semiquantitative Prussian Blue assay, nuclear magnetic resonance (^{31}P-NMR), gel permeation chromatography (GPC), and GC-MS/MS were performed to analyze lignin consumption, respectively. First, Prussian Blue assay suggested that $A_{pUI-2549}$ and $A_{pUV-2541D}$ consumed significantly more lignin than the control strain A_{pU} ($p < 0.05$, Fig. 3A). Second, lignin degradation was further confirmed by ^{31}P NMR analysis (Fig. 3B). It suggested that $A_{pUI-2549}$ and $A_{pUV-2541D}$ greatly decreased phenolic functional groups by different amounts, with the guaiacyl phenolic group decreased by the greatest amount, at more than 75%. In addition, the *p*-hydroxy-phenyl OH group was also degraded more than 30–40% by $A_{pUI-2549}$ and $A_{pUV-2541D}$, as compared to 14% degradation by A_{pU}. Other functional groups including catechol type OH and carboxylic acid OH were consumed at 25–28% by $A_{pUI-2549}$ and $A_{pUV-2541D}$, while they were decreased at 7–17% by A_{pU}, respectively. Together, this suggested $A_{pUI-2549}$ and $A_{pUV-2541D}$ was capable of more efficient lignin utilization than A_{pU}. Third, GPC analysis showed the molecular weight changes of lignin by A_{pU}, laccase, $A_{pUI-2549}$, and $A_{pUV-2541D}$, respectively. The weight average molecular weight (M_w) of lignin was decreased by A_{pU} or laccase, as compared to the blank, validating that both *P. putida* A514 and laccase play a key role in lignin degradation ($p < 0.05$, Fig. 3C and Fig. S6†). Interestingly, in contrast to A_{pU}, $A_{pUI-2549}$ and $A_{pUV-2541D}$ appeared to increase the molecular weight of lignin, especially for $A_{pUV-2541D}$ ($p < 0.05$, Fig. 3C). Considering that the M_w of laccase-only treated lignin was lower than the blank sample, $A_{pUI-2549}$ and $A_{pUV-2541D}$ should contribute to lignin fragmentation of lower mass lignin during lignin depolymerization and subsequent consumption of the low molecular lignin during lignin utilization. Thus, GC-MS/MS was subsequently carried out to analyze the soluble low molecular weight compounds in $A_{pUI-2549}$ and $A_{pUV-2541D}$ (Fig. 3D). (i) More soluble low molecular weight aromatic compounds were observed in $A_{pUI-2549}$ and $A_{pUV-2541D}$, compared to A_{pU}. These included vanillylmandelic acid (VmA), homovanillyl alcohol (HA), methylbenzoic acid (MD), 4-hydroxy-3-methoxyphenylglycol (HMP), methyl 2,4-dihydroxybenzoate (MD), and 3-hydroxy-4-methoxybenzyl alcohol (HMA) (Fig. 3D). (ii) In contrast to A_{pU}, a greater proportion of low molecular weight compounds decreased rapidly in $A_{pUI-2549}$ and $A_{pUV-2541D}$, *e.g.*, vanillylmandelic acid (VmA), homovanillyl alcohol (HA), vanillic acid (VA), guaiacol (GU) and phenol (Ph) (Fig. 3D). Among these low molecular weight compounds, vanillic acid was present in the blank and A_{pU}, at a relatively constant level. Considering that A514 can catabolize vanillic acid,[29] A_{pU} should maintain the balance between generation and consumption (Fig. S7A†). Interestingly, vanillic acid decreased rapidly in both $A_{pUI-2549}$ and $A_{pUV-2541D}$ (Fig. S7A†), suggesting that $A_{pUI-2549}$ and $A_{pUV-2541D}$ potentially

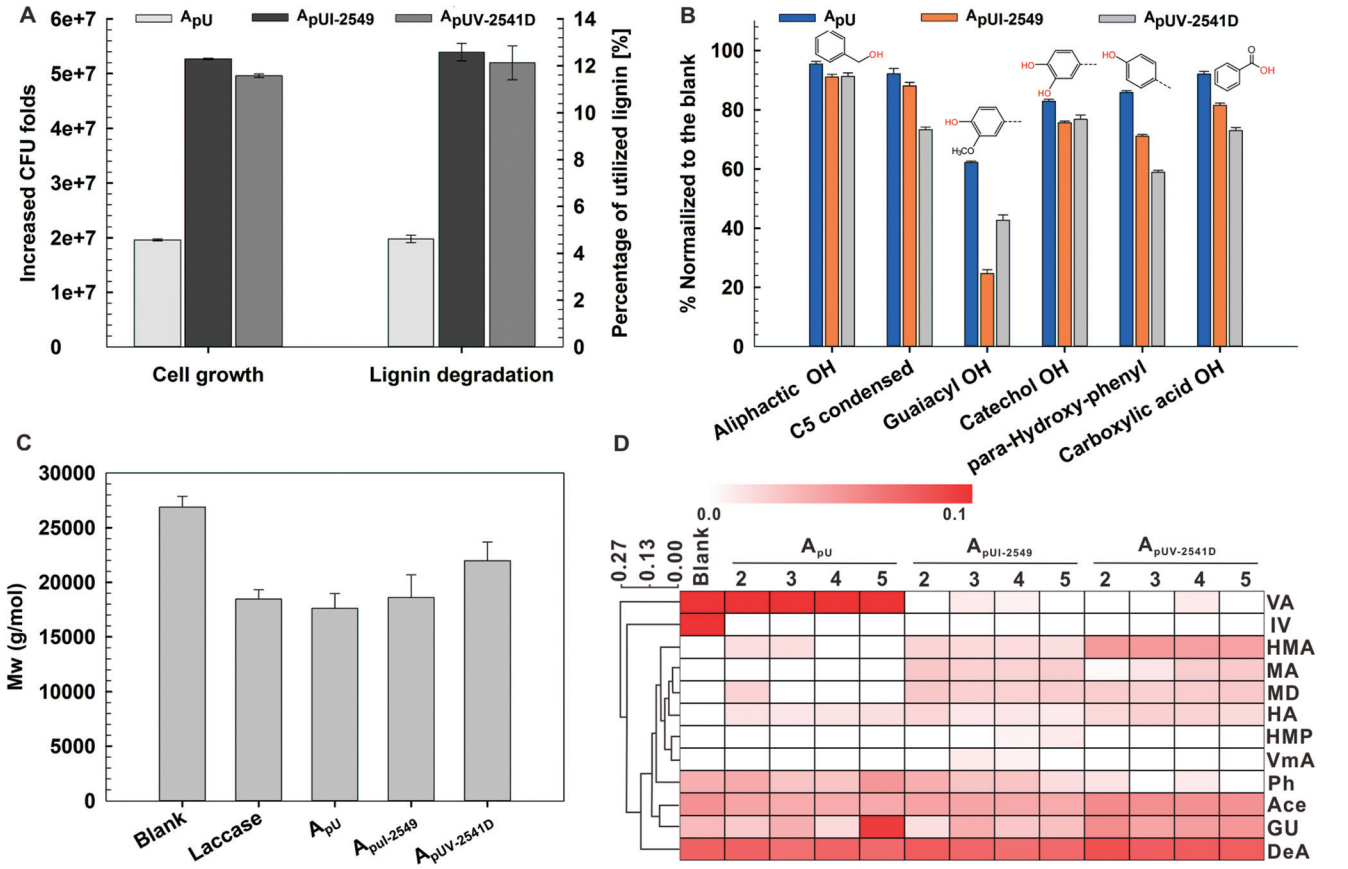

Fig. 3 The effect of laccase-A514 cells on lignin utilization. (A) The increased CFU folds and lignin degradation of $A_{pUI\text{-}2549}$ and $A_{pUV\text{-}2541D}$ in lignin-M9 rich medium. A_{pU}, which carry the empty vector, was used as the control. (B) ^{31}P NMR quantification of the functional group of lignin remaining in the media after cultivation. The hydroxyl content of lignin in the lignin rich medium (no cell blank) was set to 100% for comparison with the strains. (C) The molecular weight analysis of the lignin by GPC. M_w of the different treated lignin is presented. Blank: lignin-M9 rich medium, Laccase: 15 U mL^{-1} laccase in lignin-M9 rich medium. (D) Hierarchical cluster heatmap of the relative abundance of the aromatic compounds in the solubilized lignin solution as detected by GC-MS/MS. The presented values were normalized *via* internal standard (ethylvanillin) and represent the relative abundance of these compounds. VA: vanillic acid, IV: isovanillin, HMA: 3-hydroxy-4-methoxybenzyl alcohol, MA: methylbenzoic acid, MD: methyl 2,4-dihydroxybenzoate, HA: homovanillyl alcohol, HMP: 4 hydroxy-3-methoxyphenylglycol, VmA: vanillylmandelic acid, Ph: phenol, Ace: acetovanillone, GU: guaiacol, DeA: dehydroabietic acid.

broke this balance, accelerating vanillic acid consumption. To validate that vanillic acid was consumed, rather than being polymerized, A_{pU}, $A_{pUI\text{-}2549}$, and $A_{pUV\text{-}2541D}$ were cultured in 15 mM vanillic acid-M9 rich medium. If vanillic acid is polymerized, strains would exhibit poor cell growth, as the consumed amount of vanillic acid is positively correlated with cell density.[20] Interestingly, both $A_{pUI\text{-}2549}$ and $A_{pUV\text{-}2541D}$ showed improved cell growth over A_{pU} ($p < 0.05$, as measured by OD600). Moreover, vanillic acid more quickly decreased in $A_{pUI\text{-}2549}$ and $A_{pUV\text{-}2541D}$ cultures, as compared to A_{pU} (Fig. S7B†). In addition, compared to A_{pU}, additional peaks were not observed in the $A_{pUI\text{-}2549}$ and $A_{pUV\text{-}2541D}$ cultures by HPLC analysis. Meanwhile, obvious precipitation (*e.g.*, insoluble polymerized products) wasn't observed in the cell culture of $A_{pUI\text{-}2549}$ and $A_{pUV\text{-}2541D}$. All these indicated that no polymerized products from vanillic acid were generated. Hence, the vanilic acid was consumed as a carbon and energy source to support cell growth.

2.5 The free extracellular laccase-*P. putida* A514 system exhibited higher lignin utilization than that of immobilized laccase

On the one hand, cells producing extracellular enzymes, may prefer to retain the secreted enzymes to enhance local concentrations of metabolites. On the other hand, lignin is a large, high molecular weight polymer, and therefore the large mass transfer would limit the biocatalysis reaction between lignin and enzymes, which is potentially more challenging when enzymes are displayed at the cell surface. To compromise between local concentrations of metabolites and substrate accessibility, a mediator (acetosyringone)[35] was introduced to act as an electron carrier between laccase and lignin and the effects of lignin utilization between the bound laccase-living cell and the free laccase-living cell systems were compared. Therefore, the two systems, $A_{pUV\text{-}2541D}$ with immobilized laccase expression and $A_{pUV\text{-}2541D}$ without laccase expression

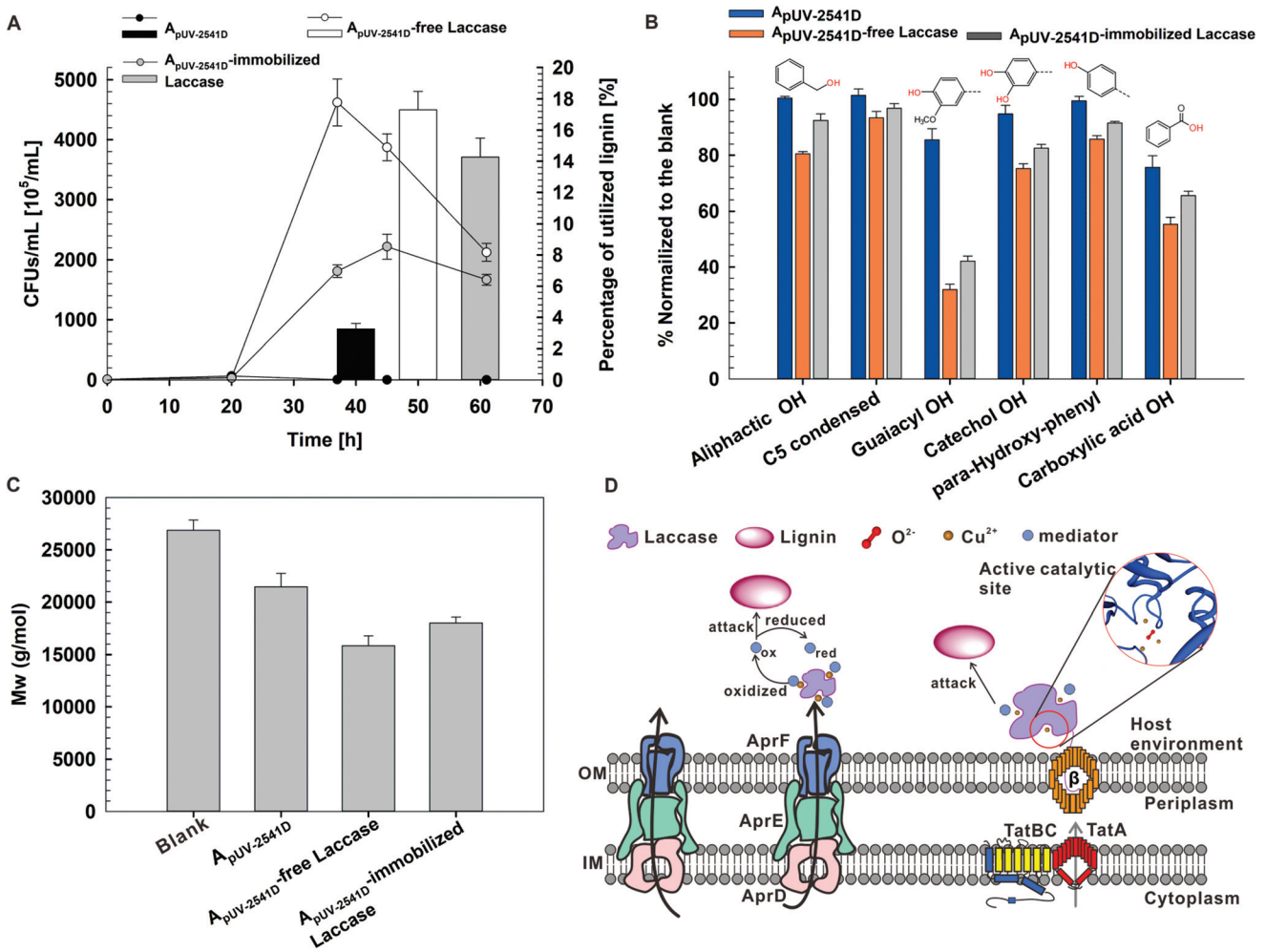

Fig. 4 Comparison the lignin utilization by extracellular free laccase-cell and cell-bound laccase-cell systems. (A) Cell growth (dotted line) and lignin degradation (bar) of $A_{pUV-2541D}$ (without laccase expression), $A_{pUV-2541D}$-free laccase mixture, and $A_{pUV-2541D}$-immobilized laccase complex. (B) ^{31}P NMR quantification of the functional group of lignin remaining in the media after cultivation. The hydroxyl content of lignin in the blank sample was set to 100% for comparison with the strains. (C) The molecular weight analysis of the lignin by GPC. $A_{pUV-2541D}$: lignin sample treated by $A_{pUV-2541D}$, which did not express laccase. Blank: lignin-M9 mineral medium. (D) Hypothesized structure model of extracellular free laccase and surface-displayed laccase, and potential catalytic mechanism with the mediator for lignin depolymerization.

plus purified laccase were incubated in lignin mineral medium, supplemented with 0.2 mM acetosyringone, at the same initial cell density (10^6 CFUs mL^{-1}) and final concentration of laccase (0.02 mg mL^{-1}), while living cells ($A_{pUV-2541D}$ without laccase expression at 10^6 CFUs mL^{-1}) in lignin mineral medium with acetosyringone was utilized as the control (Fig. 4).

First, the free laccase-$A_{pUV-2541D}$ mixture exhibited higher lignin utilization than the immobilized laccase complex by the Prussian Blue assay (17.31% *vs.* 14.27%, $p < 0.05$, Fig. 4A). Second, the ^{31}P NMR analysis further revealed that the $A_{pUV-2541D}$-free laccase mixture significantly decreased the levels of aliphactic OH, guaiacyl phenolic OH, *p*-hydroxyphenyl OH, and carboxylic acid OH groups by 69%, 15%, and 45%, respectively, as compared to 58%, 9%, and 35% degradation of those groups in the $A_{pUV-2541D}$-immobilized laccase complex (Fig. 4B, $p < 0.05$). Third, GPC analysis showed that the weight average molecular weight (M_w) of lignin was lower in the free laccase-$A_{pUV-2541D}$ mixture, as compared to the immobilized laccase-$A_{pUV-2541D}$ complex (Fig. 4C, $p < 0.05$). Fourth, the free laccase-$A_{pUV-2541D}$ mixture not only rapidly reached maximal cell density (37 h *vs.* 45 h), but also showed 2.1-fold enhancement of highest cell density over $A_{pUV-2541D}$ with immobilized laccase (Fig. 4A).

3 Discussion

3.1 Novel insights into recombinant protein secretion in *P. putida*

Extracellular production of recombinant proteins is crucial to improving microbial capacity of energy acquisition, yet this is highly challenging in Gram-negative bacteria, as secreted proteins must cross the two membranes of the cell envelope.[25,47]

Our study revealed several strategies for the secretion of a lignin-olytic enzyme in *P. putida* to counter this hurdle.

First, our study expanded the C-terminal signal peptide toolbox in TISS. Among the dedicated secretion systems, TISS continues to be the preferred system for recombinant proteins, due to its simplicity. Through TISS, many proteins in *E. coli* and *Pseudomonas* species have been successfully secreted in a single step process, without a periplasmic intermediate.[47] However, these reported extracellular recombinant proteins were primarily mediated by the limited C-terminal signal peptides from either haemolysin (HlyA) in *E. coli* or lipase (TliA) in *Pseudomonas.*[33,48] This is in sharp contrast to the numerous available N-terminal signal peptides (*e.g.*, Sec and Tat signal peptides) in the Type II and Type V secretion systems,[40,49,50] hence, greatly restricting the range of extracellular proteins production by TISS. Taking LARD3-mediated protein secretion for example, the proteins secreted *via* this system are highly negatively charged with highly acidic isoelectric points (pI < 5.5).[33] The pI of laccase is ~7, which is higher than 5.5, thus cannot be driven across the dual-membrane envelopes by LARD3 (Fig. 1B). To overcome this barrier, the C-terminal signal sequence of AprA was used to guide laccase to the surrounding medium, thereby presenting another C-terminal signal sequence in TISS for extracellular protein production, especially for proteins with higher pI values.

Second, the bio-designed AT system not only effectively secreted extracellular laccase, but also expanded the knowledge of this two-step secretion process. A two-step secretion process is also a frequently employed secretory strategy, where signal peptide-containing precursors are first transported into the periplasmic space and then transported outside the cell.[27] The bio-designed AT suggested that the N-terminal Tat signal peptide can be employed within ATs to effectively drive laccase to the periplasmic space. ATs are reported to possess N-terminal Sec signal peptides, which transport unfolded proteins across the IM, as it is more compatible with a narrow β-barrel pore structure for OM translocation than that of folded proteins.[51] Moreover, few reports have provided evidence that ATs are translocated across the IM *via* the classical Tat pathway.[52–54] Interestingly, our study suggested that the Tat signal peptide associated with the β-domain of EspP can effectively display laccase on the cell surface. We speculate that the small size of laccase may be beneficial to a secretion-competent and protease-resistant protein, which would allow laccase to efficiently traverse through the available pore. Alternatively, there might be the presence of an intermediate barrel conformation, which would exhibit a transiently larger pore size for folded passenger protein translocation.[52,55] On the other hand, the bio-designed AT also revealed that an appropriate linker region is key to efficient display of the enzyme on the cell surface. Similar to the role of an N-terminal signal peptide for IM translocation of targeted proteins, the linker domain, a region connecting the passenger domain and the β domain, is important for the translocation of proteins across the OM. Previous studies have shown that the efficiency of OM translocation decreased significantly with sequential deletion of the linker region.[45,56] Interestingly, in this study, an increased secretion efficiency and laccase activity was observed with gradual truncation of the linker region, which is contrary to previous research (Fig. 2D and Fig. S4†).[45] The linker region of EspP in *E. coli* contains the conserved motifs, *e.g.* N-terminal hydrophobic amino acids and C-terminal α-helical region, which should affect its function.[45] The amino acid sequence analysis suggested the linker region of 2541 contained the conserved C-terminal α-helical region, however the N-terminal hydrophobic amino acids were absent, possibly causing the inconsistent results (Fig. S4B†).[45] Together, the bio-designed AT, which recombined the Tat signal peptide and EspP β-domain with an appropriate linker region, not only expands the repertoire of recombinant proteins to alleviate the restriction in the secretion of proteins that fold rapidly in the cytoplasm, but also challenges the long-standing assumption that all signal peptides interact with the Sec machinery in a stereotypical fashion.

Third, the capacity of Tat protein secretory system is not a limitation for the efficient secretion of laccase. Similar to the requirement of co-expression ABC transporters in TISS, co-expression of the *tatABC* operon is a general strategy to enhance the secretion capacity in Tat protein secretory system.[35,36] Unexpectedly, our study suggested that over-expression *tatABC* did not enhance laccase activity in the periplasmic and extracellular space, possibly as the Tat pathway wasn't rapidly oversaturated in this study.

3.2 *P. putida* as a favorable cell factory for extracellular laccase secretion

Laccase is an industrially attractive biocatalyst and has numerous biotechnological applications in industry, *e.g.*, lignin valorization, bio-bleaching, and xenobiotics bioremediation.[21,57,58] The current study suggested that *P. putida* is a favorable cell factory to secrete extracellularly active laccase (Table 1).[59–65]

First, strain A514 has a high tolerance of copper toxicity. While copper is essential for laccase activity, it is also toxic to cells.[66] In Gram-positive strains, copper has mostly been introduced at the micromolar level (Table 1).[67,68] In contrast, A514 exhibited copper tolerance at millimolar levels, which contributed to the enhanced laccase activity. This could be a benefit derived from the periplasmic space in Gram-negative bacteria, which forms a natural barrier against high concentrations of copper ions in the extracellular environment.[69,70]

Second, we have developed two secretion platforms to extracellularly secrete high levels of active laccase in *P. putida* A514. On one hand, laccase can be secreted to the medium by Type I ABC transporter system when recombined with the C-terminal AprA signal peptide. On the other hand, laccase can be displayed on the cell surface by the bio-design Type V AT secretory system. Free extracellular enzymes and cell-immobilized enzymes are two common strategies utilized by microbes for protein secretion.[40,71] Free extracellular enzymes could maintain better folded conformation and enzyme activity, but lower enzyme concentrations with requirements of a large volume of cell supernatant. Cell-immobilized enzymes could increase the

Table 1 Comparison of extracellular recombinant laccase activities in microorganisms. Heterologous laccases, which were extracellularly expressed in different microbes, including Gram-negative and Gram-positive bacteria and fungi, *via* different secretion systems

Host bacteria		Laccase sources	Secretion system	Cu^{2+} [mM]	Extracellular location	Substrate	Reaction buffer	Laccase activity	Ref.
Gram-negative	*P. putida* $A_{pUI-2549}$	*S. coelicolor* A3(2)	Type I	1	Free	2.5 mM ABTS	50 mM NaOAc·HAc buffer (pH 4.5)	15.47 ± 1.37 U mL^{-1a}	This study
	P. putida $A_{pUV-2541D}$	*S. coelicolor* A3(2)	Type V	1	Cell-bound	2.5 mM ABTS	50 mM NaOAc·HAc buffer (pH 4.5)	298.64 ± 13.71 U mL^{-1} 18.67 ± 0.89 U per 10^8 cells	
	P. putida Migula AB92019	*Shigella dysenteriae* W202	Ice nucleation protein (INP)-anchored system	0.1	Cell-bound	0.5 mM ABTS	0.1 mM NaOAc·HAc buffer (pH 3.0)	7.50 U per 10^8 cells	Wang *et al.* (2012)[83]
	E. coli BL21 (DE3)	*B. subtilis* LS02	Type I Type II ND[b]	0.1	Free	0.5 mM ABTS	NM[c]	0.03 U mL^{-1} 0.01 U mL^{-1} 2.40 U mL^{-1}	Wang *et al.* (2017)[84]
Gram-positive	*Rhodococcus opacus* PD630	*S. coelicolor* A3(2)	Type II (Tat)	NM	Free	6 mM ABTS	50 mM NaOAc·HAc buffer (pH 5.0)	120.00 U mL^{-1}	Xie *et al.* (2019)[35]
	B. subtilis WB600	*B. pumilus* W3	Type II (Sec)	0.1	Free	2 mM DMP[d]	100 mM CiH_3-Na_2HPO_4-H_3BO_3 buffer (pH 7.8)	373.10 U mL^{-1}	Guan *et al.*, (2015)[58]
Fungi	*Pichia pastoris* GS115	*E. coli* K12	ND[a]	0.2	Free	2 mM ABTS	50 mM H_3Ci-Na_2HPO_4 buffer (pH 3.0)	41.00 U mL^{-1}	Ma *et al.* (2017)[59]
	Aspergillus niger	*P. cinnabarinus* I-937	Glucoamylase preprosequence	2	Free	3 mM ABTS	100 mM NaOAc·HAc buffer (pH 5.0)	2.40 U mL^{-1}	Camarero *et al.* (2012)[60]
	Pichia pastoris GS115	*Trametes trogii* BAFC 463	The Lcc3 signal peptide	1	Free	1 mM ABTS	McIlvaine buffer (pH 4.5)	5.74 U mL^{-1}	Levin *et al.* (2016)[61]
	P. pastoris X33	*Cerrena* sp. *strain* HYB07	The rLcc1 signal peptide	1	Free	0.25 mM ABTS	100 mM Na_3Ci·H_3Ci buffer (pH 3.5)	6.30 U mL^{-1}	Yang *et al.* (2015)[62]
	Pichia pastoris GS115	*P. capsici* Phyc12	The Pclac2 signal peptide	NM	Free	0.5 mM ABTS	1 M NaOAc·HAc buffer (pH 4.0)	84 U mL^{-1}	Feng *et al.* (2014)[63]
	P. pastoris X33	*basidiomycete* PM1	α-factor preproleader	3	Free	3 mM ABTS	100 mM NaOAc·HAc buffer (pH 4.0)	3.22 U mL^{-1}	Mate *et al.* (2013)[64]
	P. pastoris GS115	*Thermus thermophilus* SG0.5JP17-16	The LacTT signal peptide	0.1	Free	1 mM ABTS	50 mM NaOAc·HAc buffer (pH 4.5)	6.13 U mL^{-1}	Liu *et al.* (2015)[65]

[a] U mL^{-1}: the total enzyme activity in one milliliter batch culture broth. [b] ND: not determined. [c] NM: not mentioned. [d] DMP: 2,6 dimethoxyphenol.

local enzyme concentration, but requires additional steps to separate enzyme and cells. Two secretory types of laccase were designed to meet varied requirements in industrial applications (Table 1). For cell-bound laccase, thrombin was added to cleave the linker between the laccase and cell to recover laccase, if desired. Moreover, transcription, translation, translocation, and protein folding were coordinated to improve laccase activity and led to 15 U mL^{-1} free laccase and 300 U mL^{-1} cell-bound laccase, respectively (Table 1). Together, *P. putida*, as a Gram-negative bacterium, is an ideal candidate to produce extracellular laccase for industrial application.

3.3 Enhanced lignin utilization by a free laccase-*P. putida* system

As stated previously, limited extracellular secretion capacity represents a major hurdle in bacterial lignin degradation.[23,24] Our study demonstrated that secreted (either free or cell-bound) laccase cooperated well with *P. putida* A514 to greatly improve lignin utilization. In contrast to the untreated lignin (the blank sample), the decreased M_w of lignin by A_{pU} and laccase suggested that either laccase or *P. putida* A514 played a role in lignin degradation. Moreover, the cell growth and lignin consumption assays all validated that $A_{pUI\text{-}2549}$ and $A_{pUV\text{-}2541D}$ promoted lignin utilization. Together with these results, the GC-MS/MS analysis suggested that $A_{pUI\text{-}2549}$ and $A_{pUV\text{-}2541D}$ led to a more efficient consumption of low molecular weight compounds, which was further validated by the consumption assay of vanillic acid. The consumption of low molecular weight lignin resulted in high molecular weight lignin accounting for a greater proportion in the residual medium. Interestingly, when a mediator was introduced, the M_w of lignin by $A_{pUV\text{-}2541D}$-free laccase mixture and $A_{pUV\text{-}2541D}$-immobilized laccase complex were both lower than that of $A_{pUV\text{-}2541D}$, suggesting that a laccase-mediator system should improve high molecular weight lignin oxidation.

Retention of secreted enzymes at the surface of the producer has been thought to be advantageous, because it increases the local enzyme concentrations. Moreover, the generated products are close the cell, thus can readily be taken up.[7] Enzymatic hydrolysis of insoluble cellulose is one such example. Aerobic fungi secrete a large amount of cellulases and act in concert. In contrast, anaerobic cellulosic bacteria only need to produce a low level of cell-bound cellulosomes to hydrolyze cellulose.[10] Thus, in this study we compared the two systems for lignin degradation. Meanwhile, acetosyringone, the mediator, was introduced to overcome the steric hindrances between lignin and laccase. Interestingly, the free laccase-cell system exhibited higher lignin utilization and cell growth. It may be tentatively interpreted as the effects of both the different 3D structures of laccase and substrate accessibility. The free laccase in the medium can be folded to its optimal state, which contributes to mediator penetration into the active site. In contrast, the folding of cell-bound laccase might be hindered by restricted space, which is likely to restrict the alignment between enzyme and substrate (Fig. 4D).

In conclusion, this study provided novel insights into secreted recombinant proteins in *P. putida*, including expanding the C-terminal signal peptide toolbox in TISS and the biodesigned AT system to challenge the long-standing assumption that all signal peptides interact with the Sec machinery in AT system. Furthermore, two strategies of extracellular laccase production were developed for potential industrial applications. It is noted that the strains utilized in this study are plasmid-based with antibiotic addition to maintain strain stability. Considering further industrial applications at large scale, integrating the laccase in the genome,[72] together with the genomic activation system currently under development in *Pseudomonas*, could provide clues to overcome the issue of compatibility between strain stability (without antibiotic addition) and high laccase activity. In addition, we demonstrated that a free laccase-A514 cell system exhibited enhanced performance on kraft lignin utilization over that of cell-bound laccase complex, which seems to be contrary to the current view of bacterial polymer catabolism. This suggested that the enzyme protein structure and sufficient reaction surface is essential for biocatalysis of highly insoluble and large lignin. Thus, improved pretreatment to enhance lignin processability[72,73] would be considered to further optimize lignin biocatalysis. Moreover, lignin biodegradation is the synergistic effect of a multi-enzyme consortium. Thus, secreting the free enzyme consortium and displaying the multi-enzyme consortium on the cell surface in the future, which reflect the coordination among lignolytic enzymes, should be investigated further to understand the catalytic effects of cell-bound and free ligninolytic enzyme consortia and, thus, the rational design of biocatalysts for lignin consolidated bioprocessing.

4 Materials and methods

4.1 Bacterial strains and growth conditions

The strains used in this study are summarized in Table S1.† *Escherichia coli* Mach I strain was used for all molecular manipulations to construct plasmids. It was grown on Luria–Bertani (LB) medium at 37 °C, 180 rpm. For laccase production, *Pseudomonas putida* A514 and its recombinant strains were grown on LB medium, supplemented with 1 mM Cu^{2+} and 1 mM Fe^{2+}. For lignin degradation, A514 and its recombinant strains were cultured in M9 mineral medium, supplemented with 0.3% (w/v) alkali insoluble lignin (catalogue # 370959, Sigma-Aldrich, St Louis, MO, USA) as the sole carbon source.[23] Gentamycin (30 μg mL^{-1}) was added to the medium when culturing *P. putida* A514 recombinant strains. In addition, 2 mM xylose (final concentration) was added to induce laccase expression. Cell growth in LB was spectrophotometrically monitored by measuring the optical densities at 600 nm (OD600), whereas in the presence of 0.3% lignin, growth was monitored by colony forming units per mL (CFU mL^{-1}; cell numbers per milliliter) as previously described.[23] Briefly, to determine the number of living cells, 100 μL culture was serially diluted, spread on LB agar plates, supplemented with 30 μg mL^{-1} gentamycin for A514 recombinant strains, and incubated at 30 °C for 24 h. The number of colonies were

counted from the plates and converted to CFU mL^{-1}. All growth experiments were performed in biological triplicate.

4.2 Plasmid and strain construction

All plasmids and primers used in this study are summarized in Tables S1 and S6,† respectively. Plasmids were constructed according to standard molecular cloning protocols.[74] The laccase gene with its native tat signal peptide sequence from *S. coelicolor* A3[28] was codon optimized and synthesized in pUC57-P_{min}-tat-laccase vector by Personalbio Company (Shanghai, China). For intracellular laccase expression, the adapted laccase without N-terminal signal peptide and the P_{xylA} promoter fragments were amplified from pUC57-P_{min}-laccase and pTP_{xylA} vectors, respectively.[29] They were digested and ligated into the plasmid pUCP18-Gm[23] through *Hind*III and *Xho*I, constructing the vector pUlac. For extracellular laccase expression *via* TISS, the 3.6 kb PCR fragment containing the *aprDEF* genes was amplified from *P. putida* A514 genomic DNA and digested with *Xba*I and *Sac*I. Meanwhile, the promoter P_{min} was digested from the vector pUC57-P_{min}-tat-laccase by *Hind*III and *Xba*I. These two fragments were subsequently ligated into the plasmid pUCP18-Gm through *Hind*III and *Sac*I, generating the plasmid pUI. Next, P_{xylA}, laccase with N-terminal His·tag, the C-terminal signal sequence of either 2539 or 2549 (amplified from A514 genome by PCR) and T1/T2 terminators (amplified from pPROBE-GT[75] by PCR) were fused through gene splicing by overlap extension (SOE) PCR to produce the 3.1 kb PCR fragment. This fragment was digested with *Hind*III and *Xho*I, and cloned into the pUI to construct plasmids pUI-2539 and pUI-2549, respectively. In addition, the His·tag-laccase-C-terminal signal sequence of 2549-T1/T2 terminator cassette was generated by SOE PCR, digested, and cloned into the pUI through *Sma*I and *Xho*I to construct pUI-rnb, as the control vector in TISS strategy. For extracellular laccase expression *via* AT in TVSS, (i) the N-terminal signal peptides were obtained by PCR amplification, using plasmids pGT-p1099-oprI-dyp2, pGT-p1099-pelB-dyp2, pUC57-P_{min}-tat-laccase, and A514 genome as the template, respectively.[20] These included oprI, pbp, pelB, tat from *S. coelicolor* A3 laccase, and A514 native tat signal peptides (0383, 0620, 1543, 1921, 2816, 4529, 4580) (Table S1 and Table S6†). Subsequently, those signal peptides were fused with laccase containing His·tag at the C-terminus and the promoter P_{xylA} fragments by SOE PCR, respectively and then ligated into pPROBE-GT through *Hind*III and *Kpn*I, generating the vectors pGoprI, pGpbp, pGpelb, pGtat, pG0380, pG0620, pG1543, pG1921, pG2816, pG4529, and pG4580 (Table S1†). Finally, the P_{xylA}::2816-His·tag-laccase cassette was ligated into the pUCP18-Gm *via* *Hind*III and *Xho*I to construct pU2816. (ii) Four β domain sequences from 1761, 2541, 3548, and 4947 were amplified from the A514 genome by PCR and ligated into pU2816 through *Kpn*I and *Xho*I, generating the corresponding recombinant AT vectors, *e.g.*, pUV-2541A (Table S1†). Similarly, pUV-2541B, pUV-2541C and pUV-2541D that contained sequentially deleted linker regions of 2541 were constructed according to the same procedures. (iii) To follow laccase secretion with different linker regions, an epitope tag containing the Myc epitope, His epitope, and thrombin protease recognition sequence (MHT) was fused to the laccase gene by SOE PCR and ligated to pUV-2541A, pUV-2541B, pUV-2541C and pUV-2541D through *Sma*I and *Kpn*I, generating pUV-MHT-Lac-2541A, pUV-MHT-Lac-2541B, pUV-MHT-Lac-2541C, and pUV-MHT-Lac-2541D, respectively. Meanwhile, MHT epitope was fused to the 2816 signal peptide and then cloned into pUV-2541A, pUV-2541B, pUV-2541C and pUV-2541D through *Sma*I and *Kpn*I, respectively, to replace the laccase gene, constructing the control vectors pUV-MHT-2541A, pUV-MHT-2541B, pUV-MHT-2541C and pUV-MHT-2541D. (iv) The P_{van}::*tatABC* or P_{min}::*tatABC* expression cassettes were amplified by PCR and ligated into pU2816 and pUV2541D through *Hind*III and *BamH*I, respectively, to construct the vectors pUV-ABC-2816, pUVM-ABC-2816, pUVV-ABC-2541D and pUVM-ABC-2541D, respectively. (iv) To release the cell-bound laccase, the thrombin cleavage site was fused to the C-terminus of 2816-his-laccase fragment by PCR and cloned into pUV-2541D by *Sma*I and *Kpn*I, constructing the vector pUV-thromobin-2541D. All plasmids were verified by DNA sequencing for further studies.

4.3 Extraction of the protein fractions in cytoplasmic, periplasmic and extracellular space

Each recombinant A514 strain was grown at 25 °C, 150 rpm in LB medium, supplemented with 30 μg mL^{-1} gentamicin. Xylose was added to induce the laccase expression when OD600 reached ~ 1.0. The cells were collected by centrifugation (8000*g*, 4 °C, 10 min) when OD600 was ~ 6.5. The supernatants were collected as the extracellular free protein fractions. In addition, the cell pellets were washed three times and resuspended in PBS buffer (pH 7.4). The washed suspension was adjusted to an OD600 < 2.0 and collected as surface-displayed protein fractions. Meanwhile, parts of the collected cell pellets were used to extract the periplasmic and cytoplasmic protein fractions. Periplasmic proteins were extracted as previously described.[23] Briefly, the cell pellets were resuspended in buffer A (50 mM Tris–HCl (pH 8.0), 20% sucrose and 1 mM EDTA (pH 8.0)), incubated (RT, 20 min), centrifuged (8000*g*, 10 min, 4 °C), and resuspended in ice-cold 5 mM $MgSO_4$ buffer (pH 6.0). After incubation at 4 °C for 20 min, the resuspended solutions were centrifuged (8000*g*, 10 min, 4 °C) and the supernatants were collected as the periplasmic extracts.[23] For cytoplasmic proteins extraction, the collected cell pellets were resuspended in PBS buffer (pH 7.4) and extracted by sonication (150 W, on 1 S and off 1 S for 5 min) as previously described.[23] The lysates were centrifuged (13 000*g*, 4 °C, 5 min) and supernatants were collected as the cytoplasmic laccase cocktail. The collected proteins from cytoplasmic, periplasmic, and extracellular space were used for 12% gel SDS-PAGE separation and laccase activity analysis. All experiments were performed in biological triplicate.

4.4 Laccase activity assay

The enzymatic activity assays were performed at 25 °C and monitored by a Synergy 2 microplate reader (BioTek, Vermont, USA). Laccase activity, was measured *via* oxidation of 2.5 mM

(final concentration) ABTS (2,2′-azino-bis(3-ethylthiazoline-6-sulfonate), Aladdin, Shanghai, China) in 50 mM acetate buffer (pH 4.5) at 420 nm (ε420 = 36 000 M^{-1} cm^{-1}).[35,76] One unit of laccase activity was defined as the amount of enzyme that oxidized 1 μmol of ABTS per min.[77] For extracellular laccase activity, the sample from A_{pUlac} was employed as the blank control to eliminate the interference of the background enzyme activity. For intracellular laccase activity, the sample from either A_{pU} or A_{pGT} was employed as the blank control. All enzymatic assays were performed in biological triplicate and technical duplicate.

4.5 Optimization of laccase activity by the one variable at a time method (OVAT)

The recombinant intracellular, periplasmic, and extracellular (free and attached) laccase activity was optimized at the transcriptional, translational, and protein folding levels by the classical OVAT method. This included expression vectors with different replicons (pPROBE-GT and pUCP18-Gm), promoters, xylose induction timing points, the concentrations and time points of added metal ions (Mn^{2+}, Cu^{2+}, Fe^{2+}), pH (5.0–8.0), culture temperature (20–30 °C), agitation rates (50–250 rpm), and incubation time (24–72 h) (Tables S2–S4†). For each condition, recombinant A514 strains were grown in LB medium with 30 μg mL^{-1} gentamicin. Cells were collected by centrifugation (8000*g*, 4 °C, 15 min) and the laccase activities were examined. A_{pGT} and A_{pU} were cultivated under the same growth condition as the blank controls. All experiments were performed in biological triplicate and technical duplicate.

4.6 ELISA Quantitation of laccase secretion when combined with different linker lengths of 2541

Each single colony of the A514 recombinant strains with c-myc epitope was grown in 5 mL LB cultures supplemented with 30 μg mL^{-1} gentamycin overnight to reach the stationary phase. Subsequently, it was inoculated at 0.5% into 20 mL LB medium with gentamycin and cultured at 25 °C, 150 rpm. When OD600 was ~1.0, 2 mM xylose was added to induce c-myc epitope and laccase expression for a total of 70 h. Afterwards the culture was centrifuged (3000*g*, 4 °C, 20 min), resuspended in the same volume of PBS buffer and vortexed for 5 minutes to break the connection between cell membrane and protein. The supernatants were collected by centrifugation (3000*g*, 4 °C, 20 min). ELISA assays were performed based on the Mouse c-myc ELISA Kit protocol (Affandi, China, A8814).

4.7 Optimization the cell growth and lignin utilization of $A_{pUI\text{-}2549}$ and $A_{pUV\text{-}2541D}$ in lignin-M9 rich medium by OVAT method

Each seed culture of A_{pU}, $A_{pUI\text{-}2549}$, and $A_{pUV\text{-}2541D}$ was prepared by inoculating a single colony into 5 mL LB medium and incubating at 30 °C and 200 rpm. When stationary phase was reached, 3 mL of each strain was harvested by centrifugation and resuspended in 1 mL M9 mineral medium. The appropriate volume of resuspended cells was inoculated to 100 mL M9 mineral medium with 0.3% lignin and cultured at 28 °C and 150 rpm. During the cultivation, six parameters were investigated by classical OVAT method to optimize cell growth and lignin utilization, including the time points for 20 μM $CuSO_4$ introduction, yeast extract concentrations (0–0.1%), inducer xylose concentrations (0–12 mM), NH_4Cl concentrations (0–0.1%), and inoculum size (10^3–10^5 CFU mL^{-1}) (Table S5†).

After optimization, the cell growth of A_{pU}, $A_{pUI\text{-}2549}$, and $A_{pUV\text{-}2541D}$ in M9-lignin rich medium was monitored by colony forming units per mL, while their lignin degradation was examined by Prussian Blue assay, NMR analysis, GPC, and GC-MS/MS. Laccase, which was purified from $A_{pUV\text{-}2541D}$, was added to the lignin-M9 rich medium at the final concentration of 15 U mL^{-1} as the control. All growth experiments were performed in biological triplicate.

4.8 The cell growth and vanillic acid utilization of $A_{pUI\text{-}2549}$ and $A_{pUV\text{-}2541D}$ in vanillic acid-M9 rich medium

A_{pU}, $A_{pUI\text{-}2549}$, and $A_{pUV\text{-}2541D}$ were cultured in 15 mM vanillic acid-M9 rich medium at 28 °C, 150 rpm. 2 mM xylose was added at 8 h, while CuSO4 was added at 22 h. Cell growth was spectrophotometrically monitored by measuring the optical densities at 600 nm (OD600). The concentrations of vanillic acid in the medium were measured by HPLC, as previously described.[72] Briefly, each culture supernatant was diluted 1 : 20 with 0.2% acetic acid and analyzed by HPLC using a Thermo UltiMate 3000 HPLC system equipped with Thermo Acclaim 120 C18 (4.6 mm × 250 mm, 5 μm) column. The flow rate was 1 mL min^{-1} and the absorbance was measured at 231 nm for 25 min.

To investigate whether polymerized products were generated by $A_{pUI\text{-}2549}$ and $A_{pUV\text{-}2541D}$, the culture supernatants of A_{pU}, $A_{pUI\text{-}2549}$, and $A_{pUV\text{-}2541D}$ after 48 h cultivation were collected by centrifugation (10 000*g*, 10 min) and filtered by 0.22 μm filter. HPLC analysis was conducted using a ZOBRAX SB-C18 reverse phase column (4.6 mm × 150 mm, 5 μm), at a flow rate of 0.5 mL min^{-1}, with monitoring at 280 nm. The gradients were as follows: 20%–30% MeOH/H_2O over 5 min, 30%–50% MeOH/H_2O from 5 to 12 min, and 50%–80% MeOH/H_2O from 12 to 26 min[78] All of the samples were prepared and analyzed in biological triplicate.

4.9 Comparison the effects between free laccase and cell-bound laccase of the laccase-*P. putida* A514 on microbial lignin utilization

First, the extracellular laccase protein in $A_{pUI\text{-}2549}$ and $A_{pUV\text{-}2541D}$ was quantified. 20 mL seed cultures of $A_{pUI\text{-}2549}$ and $A_{pUV\text{-}2541D}$ were cultured in LB medium at 30 °C and 200 rpm for ~20 h. Next, 0.5% cell cultures were transferred to 300 mL LB medium, supplemented with 1 mM Fe^{2+} and 1 mM Cu^{2+} and cultured at 25 °C and 150 rpm. When the OD600 was ~1.0, xylose was added to a final concentration of 2 mM. The $A_{pUI\text{-}2549}$ supernatants were collected by centrifugation (13 000*g*, 4 °C, 15 min) as crude extracellular laccase. $A_{pUV\text{-}2541D}$ cell pellets were collected by centrifugation, resuspended in digestion buffer (20 mM Tris-HCl, 150 mM NaCl,

pH 8.0) and digested with 30 U thrombin (Solarbio, China) at 30 °C. After 12 h, the cell-bound laccase was released to the supernatant and collected by centrifugation. Subsequently, the His-tagged extracellular laccase from either $A_{pUI\text{-}2549}$ or $A_{pUV\text{-}2541D}$ was purified by Ni-NTA column (Takara) as previously described.[23] The purified laccase proteins were concentrated by using Amicon Ultra centrifugal filter devices (Millipore, United States) and quantified by BCA method.[79]

Second, the two laccase-cell systems were compared under the same conditions. 20 mL seed solutions of $A_{pUV\text{-}2541D}$ were cultured in LB medium at 30 °C, 200 rpm. After 20 h cultivation, 0.5% cell culture was inoculated to 100 mL LB medium with 1 mM Fe^{2+} and 1 mM Cu^{2+} and cultured at 25 °C and 150 rpm under two conditions: (i) 2 mM (final concentration) xylose was added when the OD_{600} was ~1.0 to induce the cell-bound laccase expression. (ii) Culture without xylose addition. When the OD600 reached ~6.5, the cells under these two conditions were collected and resuspended in 10 mL basal salts (3 g L^{-1} KH_2PO_4, 6 g L^{-1} Na_2HPO_4, 0.5 g L^{-1} NaCl and 1 g L^{-1} NH_4Cl). Subsequently, 10^8 CFUs of $A_{pUV\text{-}2541D}$, with 2 mg cell-immobilized laccase based on above quantitative method, were cultured in fresh 100 mL M9 mineral medium supplemented with 0.3% (w/v) lignin as the sole carbon source and 0.2 mM acetosyringone as the mediator at 25 °C and 150 rpm for three days. Meanwhile, 10^8 CFUs of $A_{pUV\text{-}2541D}$ without laccase expression were also cultured under the same condition, supplemented with 2 mg purified laccase from $A_{pUI\text{-}2549}$. In addition, $A_{pUV\text{-}2541D}$ without either cell-immobilized laccase or free laccase in lignin-M9 mineral medium was used as the control, respectively. All growth experiments were performed in biological triplicate.

4.10 Lignin concentration analysis by Prussian Blue assay

After five days cultivation, lignin concentration was measured by Prussian blue assay, as previously described.[23] Briefly, residual lignin in the culture medium was completely dissolved by adjusting the pH to 12.5 with 2 M NaOH. 1.5 mL of dissolved lignin solution was mixed with 100 μL 8 mM $K_3Fe(CN)_6$ and 100 μL 0.1 M $FeCl_3$, incubated for 5 min at RT, and monitored by absorbance at 700 nm to determine the concentration of lignin.

4.11 Quantitative ^{31}P nuclear magnetic resonance (NMR) analysis of lignin

The NMR experiments were carried out using a Bruker Avance 600 MHz NMR spectrometer, according to the previously described method.[80] Residual lignin, with five days cultivation, was completely dissolved by adjusting the pH to 12.5 with 50% NaOH. After centrifugation (8000*g*, 10 min, 4 °C), lignin supernatant solution was collected and its pH was adjusted to 2 to precipitate lignin. The lignin deposit was collected by centrifugation (5000*g*, 10 min, 25 °C) and freeze-dried for a minimum of 24 h.[29] Lignin (25 mg) was dissolved in a solvent of pyridine/$CDCl_3$ (1.6/1.0 v/v, 550 μL) containing chromium acetylacetonate (relaxation agent) and *endo*-*N*-hydroxy-5-norbornene-2,3-dicarboximide (NHND, internal standard), and then derivatized with 2-chloro-4,4,5,5-tetramethyl-1,3,2-dioxaphospholane. The spectrum was acquired using an inverse-gated decoupling pulse sequence (Waltz-16), a 90° pulse, and a 25 s pulse delay. 128 scans were accumulated for each sample. NMR data were processed using the TopSpin 4.0 software (Bruker BioSpin) software packages. All experiments were performed in biological triplicate.

4.12 Gel permeation chromatography (GPC) analysis of lignin

The molecular weight of the lignin was analyzed by GPC, as previously described.[14,72] Briefly, lignin was prepared by the same procedure as for NMR analysis. The lignin (20 mg) was first acetylated by incubating with acetic anhydride/pyridine (1 : 1 v/v, 2.0 mL) in a sealed flask under an insert atmosphere at RT for 24 h. The sample was diluted with 20 mL of ethanol and stirred for 30 min. The ethanol in each sample was removed with a rotary evaporator, followed by drying in a vacuum oven at 40 °C. Subsequently, each acetylated lignin sample was dissolved in tetrahydrofuran (1.0 mg mL^{-1}) and filtered through a 0.45 μm filter. The molecular weight distributions of the acetylated lignin samples were analyzed on an GPC Waters 1525 system equipped with four Waters Styragel columns (HR1, HR2, HR4, HR6) and a waters 2414 detector. Tetrahydrofuran was used as the mobile phase in GPC analysis at the 1.0 mL min^{-1} flow rate. In addition, a standard polystyrene sample was used for calibration. All experiments were performed in biological triplicate.

4.13 GC-MS/MS analysis of the degraded lignin products

The solubilized monomer and oligomer compounds, released through lignin depolymerization, were analyzed by GC-MS/MS as previously described.[14] 3 mL cell samples of A_{pU}, $A_{pUI\text{-}2549}$, and $A_{pUV\text{-}2541D}$ in M9-lignin rich medium at 2, 3, 4 and 5 cultivation days were centrifuged (13 000*g*, 25 °C, 8 min) and the collected supernatants were extracted with 9 mL of ethyl acetate. The organic layer was collected and dewatered using anhydrous sodium sulfate. Next, 2 mL of dewatered solution was collected by centrifugation (8000*g*, 25 °C, 10 min) and dried under nitrogen gas stream. The dried residue was mixed with 100 μL dioxane containing ethylvanilline (3-methoxyphenylacetophenone) as an internal standard (i.s.) (33 mg mL^{-1}), 10 μL pyridine, and 50 μL trimethylsilyl [BSTFA (*N*,*O*-bis(trimethylsilyl) trifluoroacetamide) and TMCS],[81,82] and then was incubated at 60 °C for 15 min with periodic shaking to completely dissolve the residue. Subsequently, 100 μL silylated compounds was 10-fold diluted with hexane and injected into an Agilent Technologies 7000D GC-MS equipped with a HP-5MS column (thickness 0.25 μm; length 30 m; diameter 0.25 mm). The column temperature program was set as 50 °C hold for 5 min, 50–300 °C (10 °C min^{-1}, hold time: 5 min). The compounds were identified by comparison with the GC-MS library database (NIST08s). The abundances of compounds were divided by the abundance of the internal standard within the sample and thus represented relative abundance of the compounds.

Author contributions

L.L. conceived and designed the experiments. L.C., L.L. and H.S. performed the experiments. L.L. and L.C. analyzed the data. L.L., J.Z., and N.J. wrote the paper. H.W. and Z.Z. contributed reagents and analysis tools. All authors read and approved the final manuscript.

Conflicts of interest

The authors declare that they have no conflicts of interest.

Acknowledgements

This work was supported by the National Natural Science Foundation of China (91951116), National Key Research and Development Project (2019YFA0606704) and Fundamental Research Funds of Shandong University (2019GN101). The funders had no role in the study design, data collection and analysis, decision to publish, or preparation of the manuscript. We would like to thank Xiaoju Li from Shandong University core facilities for life and environmental Sciences for their help and guidance in NMR assay.

References

1 T. S. Bianchi, *Proc. Natl. Acad. Sci. U. S. A.*, 2011, **108**, 19473–19481.
2 S. Xie, R. Syrenne, S. Sun and J. S. Yuan, *Curr. Opin. Biotechnol*, 2014, **27**, 195–203.
3 D. Floudas, M. Binder, R. Riley, K. Barry, R. A. Blanchette, B. Henrissat, A. T. Martinez, R. Otillar, J. W. Spatafora, J. S. Yadav, A. Aerts, I. Benoit, A. Boyd, A. Carlson, A. Copeland, P. M. Coutinho, R. P. de Vries, P. Ferreira, K. Findley, B. Foster, J. Gaskell, D. Glotzer, P. Gorecki, J. Heitman, C. Hesse, C. Hori, K. Igarashi, J. A. Jurgens, N. Kallen, P. Kersten, A. Kohler, U. Kues, T. K. Kumar, A. Kuo, K. LaButti, L. F. Larrondo, E. Lindquist, A. Ling, V. Lombard, S. Lucas, T. Lundell, R. Martin, D. J. McLaughlin, I. Morgenstern, E. Morin, C. Murat, L. G. Nagy, M. Nolan, R. A. Ohm, A. Patyshakuliyeva, A. Rokas, F. J. Ruiz-Duenas, G. Sabat, A. Salamov, M. Samejima, J. Schmutz, J. C. Slot, F. St John, J. Stenlid, H. Sun, S. Sun, K. Syed, A. Tsang, A. Wiebenga, D. Young, A. Pisabarro, D. C. Eastwood, F. Martin, D. Cullen, I. V. Grigoriev and D. S. Hibbett, *Science*, 2012, **336**, 1715–1719.
4 G. de Gonzalo, D. I. Colpa, M. H. Habib and M. W. Fraaije, *J. Biotechnol.*, 2016, **236**, 110–119.
5 H. G. Hoppe, in *Microbial enzymes in aquatic environments*, ed. I. C. R.J., Springer New York, 1991, pp. 60–83.
6 C. Arnosti, *Ann. Rev. Mar. Sci.*, 2011, **3**, 401–425.
7 F. Putker, R. Tommassen-van Boxtel, M. Stork, J. J. Rodriguez-Herva, M. Koster and J. Tommassen, *Environ. Microbiol.*, 2013, **15**, 2658–2671.
8 G. J. Velicer, *Trends Microbiol.*, 2003, **11**, 330–337.
9 S. Y. Ding, Q. Xu, M. Crowley, Y. Zeng, M. Nimlos, R. Lamed, E. A. Bayer and M. E. Himmel, *Curr. Opin. Biotechnol*, 2008, **19**, 218–227.
10 C. You, X. Z. Zhang, N. Sathitsuksanoh, L. R. Lynd and Y. H. Zhang, *Appl. Environ. Microbiol.*, 2012, **78**, 1437–1444.
11 B. Wu, J. Gaskell, B. W. Held, C. Toapanta and D. S. Hibbett, *Appl. Environ. Microbiol.*, 2018, **84**, e00991–e00918.
12 S. Moraïs, Y. Barak, J. Caspi, Y. Hadar, R. Lamed, Y. Shoham, D. B. Wilson and E. A. Bayer, *mBio*, 2010, **1**, e00285–e00210.
13 Y. Lu, Y. H. Zhang and L. R. Lynd, *Proc. Natl. Acad. Sci. U. S. A.*, 2006, **103**, 16165–16169.
14 S. Xie, Q. Sun, Y. Pu, F. Lin and J. S. Yuan, *ACS Sustainable Chem. Eng.*, 2016, **5**, 2215–2223.
15 X. Zang, M. Liu, Y. Fan, J. Xu, X. Xu and H. Li, *Biotechnol. Biofuels*, 2018, **11**, 51.
16 W. T. Beeson, V. V. Vu, E. A. Span, C. M. Phillips and M. A. Marletta, *Annu. Rev. Biochem.*, 2015, **84**, 923–946.
17 J. Becker and C. Wittmann, *Biotechnol. Adv.*, 2019, **37**, 107360.
18 E. C. Moraes, T. M. Alvarez, G. F. Persinoti, G. Tomazetto, L. B. Brenelli, D. A. A. Paixao, G. C. Ematsu, J. A. Aricetti, C. Caldana, N. Dixon, T. D. H. Bugg and F. M. Squina, *Biotechnol. Biofuels*, 2018, **11**, 018–1073.
19 T. D. Bugg, M. Ahmad, E. M. Hardiman and R. Singh, *Curr. Opin. Biotechnol*, 2011, **22**, 394–400.
20 L. Lin, Y. Cheng, Y. Pu, S. Sun, X. Li, M. Jin, E. A. Pierson, D. C. Gross, B. E. Dale, S. Y. Dai, A. J. Ragauskas and J. S. Yuan, *Green Chem.*, 2016, **18**, 5536–5547.
21 J. G. Linger, D. R. Vardon, M. T. Guarnieri, E. M. Karp, G. B. Hunsinger, M. A. Franden, C. W. Johnson, G. Chupka, T. J. Strathmann, P. T. Pienkos and G. T. Beckham, *Proc. Natl. Acad. Sci. U. S. A.*, 2014, **111**, 12013–12018.
22 D. Salvachua, E. M. Karp, C. T. Nimlos, D. R. Vardon and G. T. Beckham, *Green Chem.*, 2015, **17**, 4951–4967.
23 L. Lin, X. Wang, L. Cao and M. Xu, *Environ. Microbiol.*, 2019, **21**(5), 1847–1863.
24 C. Zhao, S. Xie, Y. Pu, R. Zhang, F. Huang, A. J. Ragauskas and J. S. Yuan, *Green Chem.*, 2016, **18**, 1306–1312.
25 R. Chen, *Biotechnol. Adv.*, 2012, **30**, 1102–1107.
26 D. Salvachúa, A. Z. Werner, I. Pardo, M. Michalska, B. A. Black, B. S. Donohoe, S. J. Haugen, R. Katahira, S. Notonier, K. J. Ramirez, A. Amore, S. O. Purvine, E. M. Zink, P. E. Abraham, R. J. Giannone, S. Poudel, P. D. Laible, R. L. Hettich and G. T. Beckham, *Proc. Natl. Acad. Sci. U. S. A.*, 2020, **117**, 9302–9310.
27 T. R. Costa, C. Felisberto-Rodrigues, A. Meir, M. S. Prevost, A. Redzej, M. Trokter and G. Waksman, *Nat. Rev. Microbiol.*, 2015, **13**, 343–359.

28 S. Majumdar, T. Lukk, J. O. Solbiati, S. Bauer, S. K. Nair, J. E. Cronan and J. A. Gerlt, *Biochemistry*, 2014, **53**, 4047–4058.
29 X. Wang, L. Lin, J. Dong, J. Ling, W. Wang, H. Wang, Z. Zhang and X. Yu, *Appl. Environ. Microbiol.*, 2018, **84**, 01469–01418.
30 P. Delepelaire, *Biochim. Biophys. Acta, Mol. Cell Res.*, 2004, **1694**, 149–161.
31 F. Duong, C. Soscia, A. Lazdunski and M. Murgier, *Mol. Microbiol.*, 2010, **11**, 1117–1126.
32 J. Ryu, U. Lee, J. Park, D. H. Yoo and J. H. Ahn, *Appl. Environ. Microbiol.*, 2015, **81**, 1744–1753.
33 H. Byun, J. Park, S. C. Kim and J. H. Ahn, *J. Biol. Chem.*, 2017, **292**, 19782–19791.
34 E. Kawai, A. Idei, H. Kumura, K. Shimazaki, H. Akatsuka and K. Omori, *Biochim. Biophys. Acta*, 1999, **3**, 377–382.
35 S. Xie, S. Sun, F. Lin, M. Li, Y. Pu, Y. Cheng, B. Xu, Z. Liu, L. da Costa Sousa, B. E. Dale, A. J. Ragauskas, S. Y. Dai and J. S. Yuan, *Adv. Sci.*, 2019, **6**, 3.
36 F. J. Mergulhao, D. K. Summers and G. A. Monteiro, *Biotechnol. Adv.*, 2005, **23**, 177–202.
37 M. Kumar, A. Mishra, S. S. Singh, S. Srivastava and I. S. Thakur, *Int. J. Biol. Macromol.*, 2018, **115**, 308–316.
38 J. D. Bendtsen, H. Nielsen, D. Widdick, T. Palmer and S. Brunak, *BMC Bioinf.*, 2005, **6**, 1471–2105.
39 S. D. Branston, C. F. Matos, R. B. Freedman, C. Robinson and E. Keshavarz-Moore, *Biotechnol. Bioeng.*, 2012, **109**, 983–991.
40 W. S. Jong, A. Sauri and J. Luirink, *Curr. Opin. Biotechnol*, 2010, **21**, 646–652.
41 P. van Ulsen, K. M. Zinner, W. S. P. Jong and J. Luirink, *FEMS Microbiol. Lett.*, 2018, **365**, fny165.
42 Y. Kida, J. Taira, T. Yamamoto, Y. Higashimoto and K. Kuwano, *Cell. Microbiol.*, 2013, **15**, 1168–1181.
43 T. Nicolay, L. Lemoine, E. Lievens, S. Balzarini, J. Vanderleyden and S. Spaepen, *Microb. Cell Fact.*, 2012, **11**, 158.
44 X. Yuan, M. D. Johnson, J. Zhang, A. W. Lo, M. A. Schembri, L. C. Wijeyewickrema, R. N. Pike, G. H. M. Huysmans, I. R. Henderson and D. L. Leyton, *Nat. Commun.*, 2018, **9**, 1395.
45 J. J. Velarde and J. P. Nataro, *J. Biol. Chem.*, 2004, **279**, 31495–31504.
46 I. Drobnak, E. Braselmann, J. L. Chaney, D. L. Leyton, H. D. Bernstein, T. Lithgow, J. Luirink, J. P. Nataro and P. L. Clark, *Mol. Microbiol.*, 2015, **95**, 1–16.
47 Y. Ni and R. Chen, *Biotechnol. Lett.*, 2009, **31**, 1661–1670.
48 M. H. H. Lenders, S. Weidtkamp-Peters, D. Kleinschrodt, K.-E. Jaeger, S. H. J. Smits and L. Schmitt, *Sci. Rep.*, 2015, **5**, 12470.
49 I. R. Henderson, F. Navarro-Garcia, M. Desvaux, R. C. Fernandez and D. Ala'Aldeen, *Microbiol. Mol. Biol. Rev.*, 2004, **68**, 692–744.
50 P. A. Lee, D. Tullman-Ercek and G. Georgiou, *Annu. Rev. Microbiol.*, 2006, **60**, 373–395.
51 C. Albenne and R. Ieva, *Mol. Microbiol.*, 2017, **106**, 505–517.
52 K. M. Skillman, T. J. Barnard, J. H. Peterson, R. Ghirlando and H. D. Bernstein, *Mol. Microbiol.*, 2005, **58**, 945–958.
53 W. Kang'ethe and H. D. Bernstein, *Proc. Natl. Acad. Sci. U. S. A.*, 2013, **110**, E4246–E4255.
54 B. S. Weber, R. L. Kinsella, C. M. Harding and M. F. Feldman, *Trends Microbiol.*, 2017, **25**, 532–545.
55 E. Veiga, V. de Lorenzo and L. A. Fernández, *Mol. Microbiol.*, 2004, **52**, 1069–1080.
56 T. H. Yang, J. G. Pan, Y. S. Seo and J. S. Rhee, *Appl. Environ. Microbiol.*, 2004, **70**, 6968–6976.
57 D. M. Mate and M. Alcalde, *Microb. Biotechnol.*, 2017, **10**, 1457–1467.
58 Z.-B. Guan, Y. Shui, C.-M. Song, N. Zhang, Y.-J. Cai and X.-R. Liao, *Environ. Sci. Pollut. Res.*, 2015, **22**, 9515–9523.
59 X. Ma, L. Liu, Q. Li, Y. Liu, L. Yi, L. Ma and C. Zhai, *Enzyme Microb. Technol.*, 2017, **103**, 34–41.
60 S. Camarero, I. Pardo, A. I. Cañas, P. Molina, E. Record, A. T. Martínez, M. J. Martínez and M. Alcalde, *Appl. Environ. Microbiol.*, 2012, **78**, 1370–1384.
61 P. A. Campos, L. N. Levin and S. A. Wirth, *Process Biochem.*, 2016, **51**, 895–903.
62 J. Yang, T. B. Ng, J. Lin and X. Ye, *Int. J. Biol. Macromol.*, 2015, **77**, 344–349.
63 B. Z. Feng and P. Li, *Braz. J. Microbiol.*, 2014, **45**, 351–357.
64 D. M. Mate, D. Gonzalez-Perez, R. Kittl, R. Ludwig and M. Alcalde, *BMC Biotechnol.*, 2013, **13**, 38.
65 H. Liu, Y. Cheng, B. Du, C. Tong, S. Liang, S. Han, S. Zheng and Y. Lin, *PLoS One*, 2015, **10**, e0119833.
66 E. Ladomersky and M. J. Petris, *Metallomics*, 2015, **7**, 957–964.
67 S. Sondhi, P. Sharma, N. George, P. S. Chauhan, N. Puri and N. Gupta, *3 Biotech*, 2015, **5**, 175–185.
68 E. Dubé, F. Shareck, Y. Hurtubise, C. Daneault and M. Beauregard, *Appl. Microbiol. Biotechnol.*, 2008, **79**, 597–603.
69 J. H. Parmar, J. Quintana, D. Ramírez, R. Laubenbacher, J. M. Argüello and P. Mendes, *Mol. Microbiol.*, 2018, **110**, 357–369.
70 J. Quintana, L. Novoa-Aponte and J. M. Argüello, *J. Biol. Chem.*, 2017, **292**, 15691–15704.
71 G. L. Huang, T. D. Anderson and R. T. Clubb, *Bioengineered*, 2014, **5**, 96–106.
72 Y. Zhou, L. Lin, H. Wang, Z. Zhang, J. Zhou and N. Jiao, *Commun. Biol.*, 2020, **3**, 98.
73 X. Li, Y. He, L. Zhang, Z. Xu, H. Ben, M. J. Gaffrey, Y. Yang, S. Yang, J. S. Yuan, W. J. Qian and B. Yang, *Biotechnol. Biofuels*, 2019, **12**, 60.
74 J. Sambrook, E. F. Fritsch and T. Maniatis, *Molecular cloning: a laboratory manual*, *C.S.H. Laboratory*, Cold Spring Harbor, NY, USA, 1989.
75 W. G. Miller, J. H. Leveau and S. E. Lindow, *Mol. Plant-Microbe Interact.*, 2000, **13**, 1243–1250.
76 Y. Zhang, W. Dong, Z. Lv, J. Liu, W. Zhang, J. Zhou, F. Xin, J. Ma and M. Jiang, *Mol. Biotechnol.*, 2018, **60**, 681–689.
77 M. Schulze, L. Geisler, A. Majcherczyk and M. Ruhl, *AMB Express*, 2019, **9**, 36.

78 G. M. M. Rashid, C. R. Taylor, Y. Liu, X. Zhang, D. Rea, V. Fülöp and T. D. H. Bugg, *ACS Chem. Biol.*, 2015, **10**, 2286–2294.
79 J. M. Walker, *Methods Mol. Biol.*, 1994, **32**, 5–8.
80 Y. Pu, S. Cao and A. J. Ragauskas, *Energy Environ. Sci.*, 2011, **4**, 3154–3166.
81 M. Hernández-Coronado, M. Hernández, J. Rodríguez and M. Arias, *Rapid Commun. Mass Spectrom.*, 1998, **12**, 1744–1748.
82 M. Hemandez, M. J. Hernandez-Coronado, M. D. Montiel, J. Rodriguez and M. E. Arias, *J. Chromatogr. A*, 2001, **919**, 389–394.
83 W. Wang, Z. Zhang, H. Ni, X. Yang, Q. Li and L. Li, *Microb. Cell Fact.*, 2012, **11**, 75.
84 T. N. Wang and M. Zhao, *Appl. Microbiol. Biotechnol.*, 2017, **101**, 685–696.